PNAS
www.pnas.org

Supplementary Information for

A cullin-RING ubiquitin ligase promotes thermotolerance as part of the Intracellular Pathogen Response in *C. elegans*.

Johan Panek, Spencer S. Gang, Kirthi C. Reddy, Robert J. Luallen, Amitkumar Fulzele, Eric J. Bennett, Emily R. Troemel.

Emily R. Troemel
Email: etroemel@ucsd.edu

This PDF file includes:

Figures S1 to S7
Table S1 to S3
Legend for Dataset S1
SI References

Other supplementary materials for this manuscript include the following:

Dataset S1

www.pnas.org/cgi/doi/10.1073/pnas.1918417117

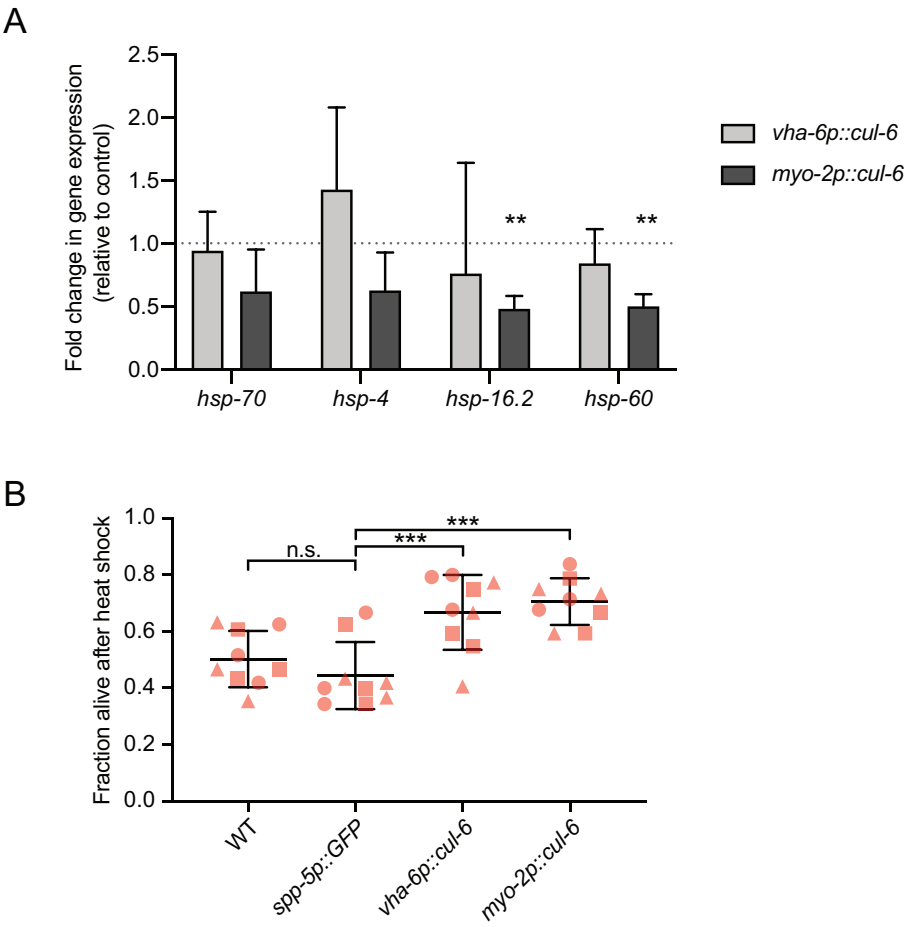

Fig. S1. Ectopic expression of *cul-6* does not induce heat shock gene expression. *(A)* qRT-PCR analysis of *hsp* gene expression in control, *vha-6p::cul-6* and *myo-2p::cul-6* L4 animals. Results shown are an average of three independent biological replicates, error bars are SD. ** $P < 0.01$, Student's t-test when compared to control. The *spp-5p::GFP* strain was chosen as a negative control because it is in the same MosSCI strain background as the *vha-6p::cul-6* and *myo-2p::cul-6* strains, and drives intestinal expression of the GFP::3xFLAG tag, which is the same tag on CUL-6 (FLAG not shown for clarity). *(B)* Survival of animals after heat shock treatment. Strains were tested in triplicate experiments, with three plates per experiment, 30 animals per plate. Each dot represents a plate and different shapes represent the experimental replicates done on different days. Mean fraction alive of the nine replicates is indicated by the black bar with error bars as SD. *** $P < 0.001$, one-way ANOVA with Tukey's *post-hoc* multiple comparisons test.

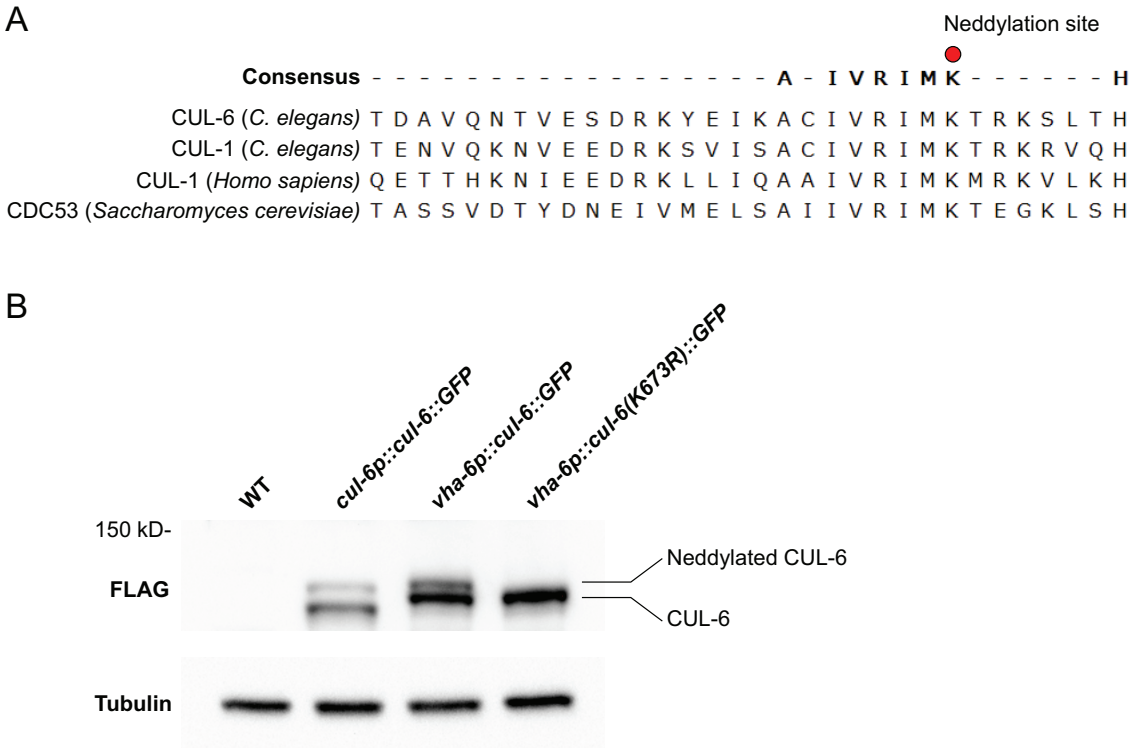

Fig. S2. Mutation of the predicted CUL-6 neddylation site suppresses CUL-6 neddylation. *(A)* Alignment of the C-terminal region of CUL-6 with other cullins. The conserved lysine residue targeted by neddylation is indicated by a red circle. *(B)* Western blot analysis on total protein lysate from wild-type animals and three strains expressing FLAG-tagged CUL-6: *cul-6p::cul-6::GFP* which expresses CUL-6::GFP::3xFLAG (116 kD), *vha-6p::cul-6::GFP* which expresses SBP_3xFLAG::GFP::CUL-6 (121 kD) and *vha-6p::cul-6(K673R)::GFP* which expresses SBP_3xFLAG::GFP::CUL-6 (121 kD) with a mutation to the lysine residue targeted for neddylation. FLAG-tagged protein was detected with anti-FLAG antibody, and anti-tubulin antibody was used as a loading control. A shift of CUL-6 covalently modified by neddylation (NED-8 = 8.6 kD) is present in *cul-6p::cul-6::GFP* and *vha-6p::cul-6::GFP* total lysate but is absent from the *vha-6p::cul-6(K673R)::GFP* neddylation mutant. The western blot shown is representative of one of two biological replicates.

A

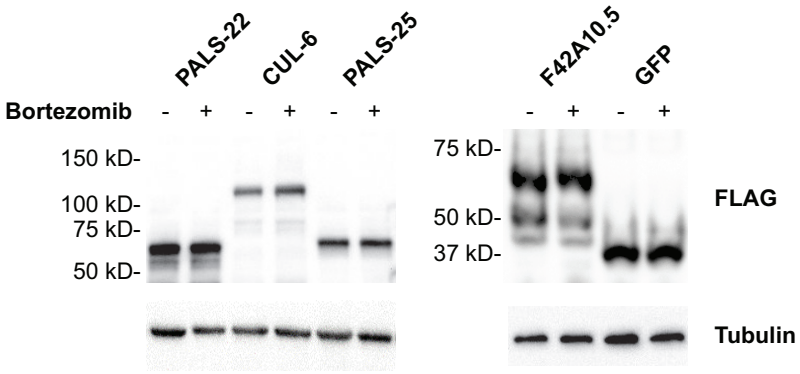

B

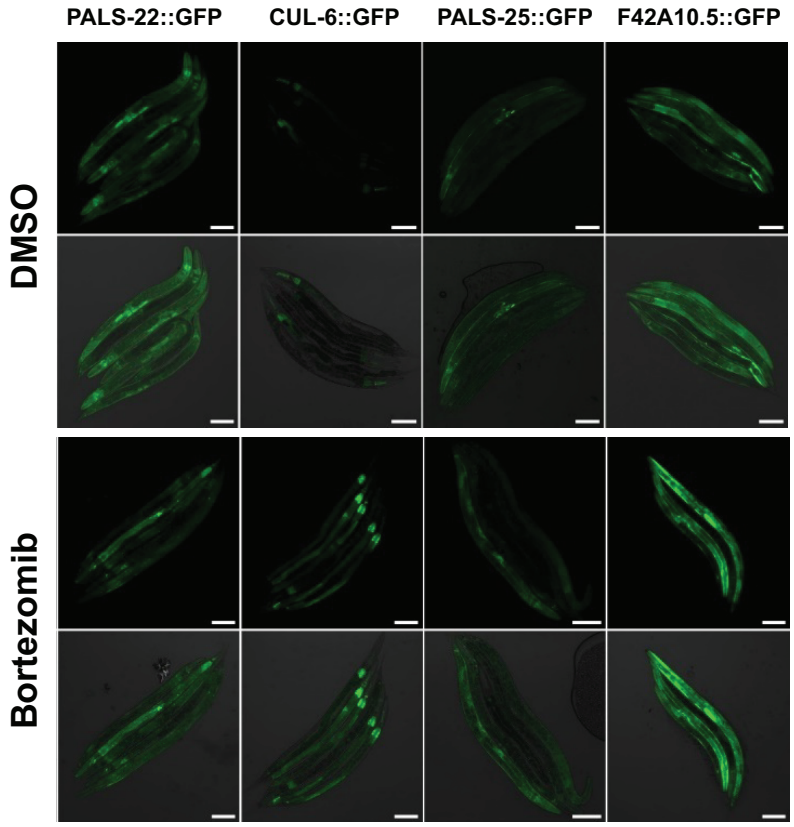

Fig. S3. Expression analysis of GFP::3xFLAG-tagged proteins used for Co-IP/MS studies. *(A)* Western blot analysis of total protein lysate from transgenic adult animals containing fosmid transgenes expressing GFP::3xFLAG-tagged protein and treated with Bortezomib or DMSO as diluent control. Proteins were detected with anti-FLAG antibody, and anti-tubulin antibody was used as a loading control. Expected sizes: CUL-6::GFP::3xFLAG (116 kD), PALS-22::GFP::3xFLAG (64.8 kD), PALS-25::GFP::3xFLAG (66.9 kD), F42A10.5::GFP::3xFLAG (61.3 kD) and GFP::3xFLAG (34 kD). *(B)* Confocal fluorescence images of L4 animals with fosmid transgenes expressing GFP-tagged proteins from endogenous promoters after exposure to DMSO or Bortezomib (diluted in DMSO). For each transgene and treatment condition top images are GFP fluorescence only and bottom images are GFP and DIC overlays. Scale bars are 100 µm.

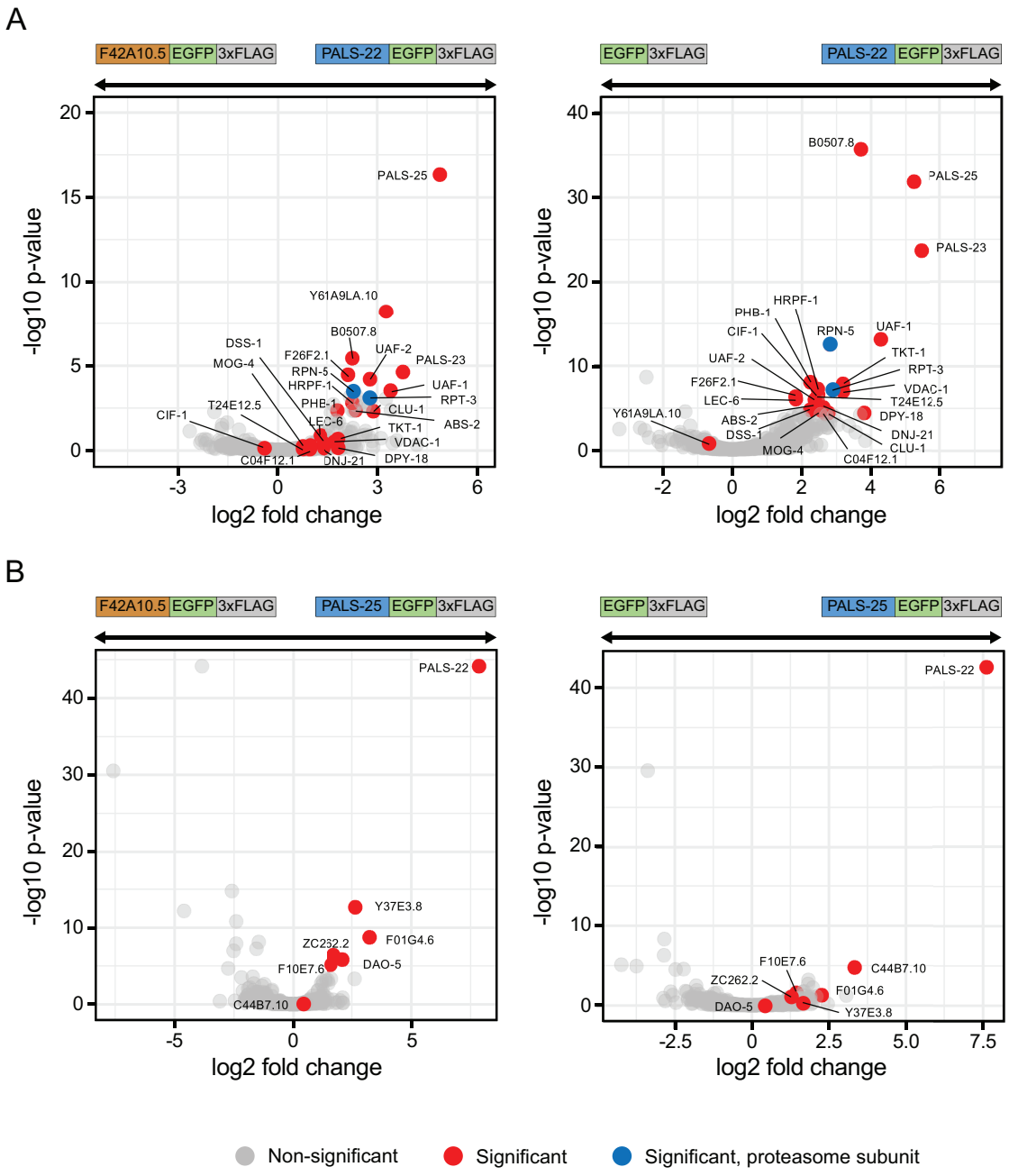

Fig. S4. Co-immunoprecipitation mass spectrometry analysis identifies binding partners for PALS-22 and PALS-25. Volcano plot of proteins significantly enriched in PALS-22 *(A)* and PALS-25 *(B)* IPs compared to F42A10.5 IP or GFP IP. Proteins significantly more abundant compared to either of the control IP's (GFP alone control or F42A10.5 control, at adjusted $P < 0.05$ and log2 fold change > 1) were considered interacting proteins (Dataset S1). Gray dots indicate non-significant proteins, red dots indicate significant proteins and blue dots indicate significant proteasome subunits.

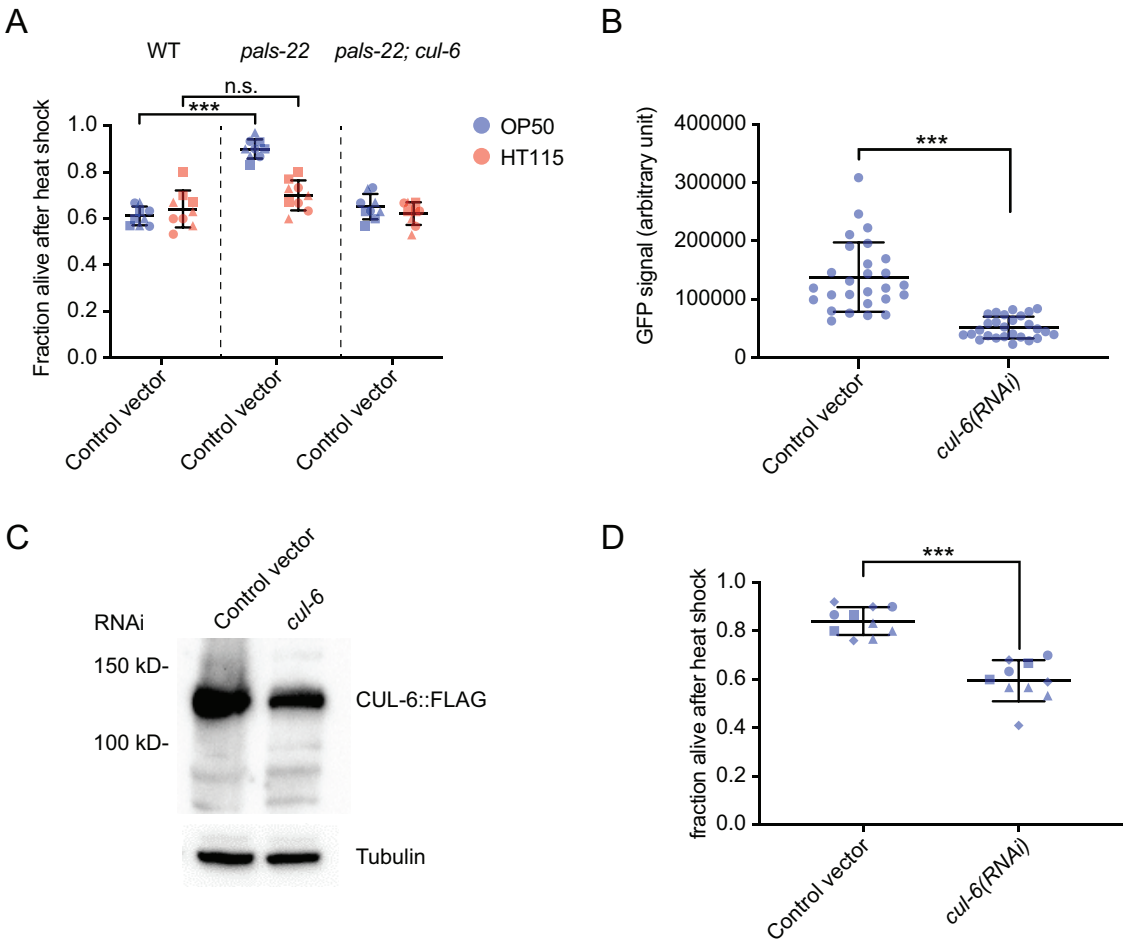

Fig. S5. Development of an RNAi system for analyzing thermotolerance in *pals-22* mutants. *(A)* Survival of animals after heat shock treatment either fed on OP50 strain (R)OP50 or HT115 *E. coli* expressing L4440 (control vector). Each dot represents a plate, and different shapes represent the experimental replicates done on different days. Mean fraction alive of the nine replicates is indicated by the black bar with errors bars as SD. *** $P < 0.001$ two-way ANOVA with Sidak's multiple comparisons test. *(B)* Quantification of GFP signal in L4 animals expressing CUL-6::GFP grown on (R)OP50 expressing either L4440 (control vector) or *cul-6* RNAi. GFP signal was measured with ImageJ in the pharynx and the first intestinal cells ring together with 3 adjacent background area and the Total Corrected Fluorescence (TCF) was calculated. Error bars are SD. *** $P < 0.001$ with Student's t-test. *(C)* Western blot analysis on total protein lysate from adult animals with fosmid transgenes expressing CUL-6::GFP::3xFLAG treated with L4440 (control vector) or *cul-6* RNAi (OP50). CUL-6::GFP::3xFLAG protein was detected with anti-FLAG antibody, and anti-tubulin antibody was used as a loading control. *(D)* Survival of *pals-22* mutants after heat shock treatment. animals fed on (R)OP50 expressing either L4440 (control vector) or *cul-6* RNAi. Each dot represents a plate, and different shapes represent the experimental replicates done on different days. Mean fraction alive of the ten replicates is indicated by the black bar with errors bars as SD. *** $P < 0.001$ with Student's t-test.

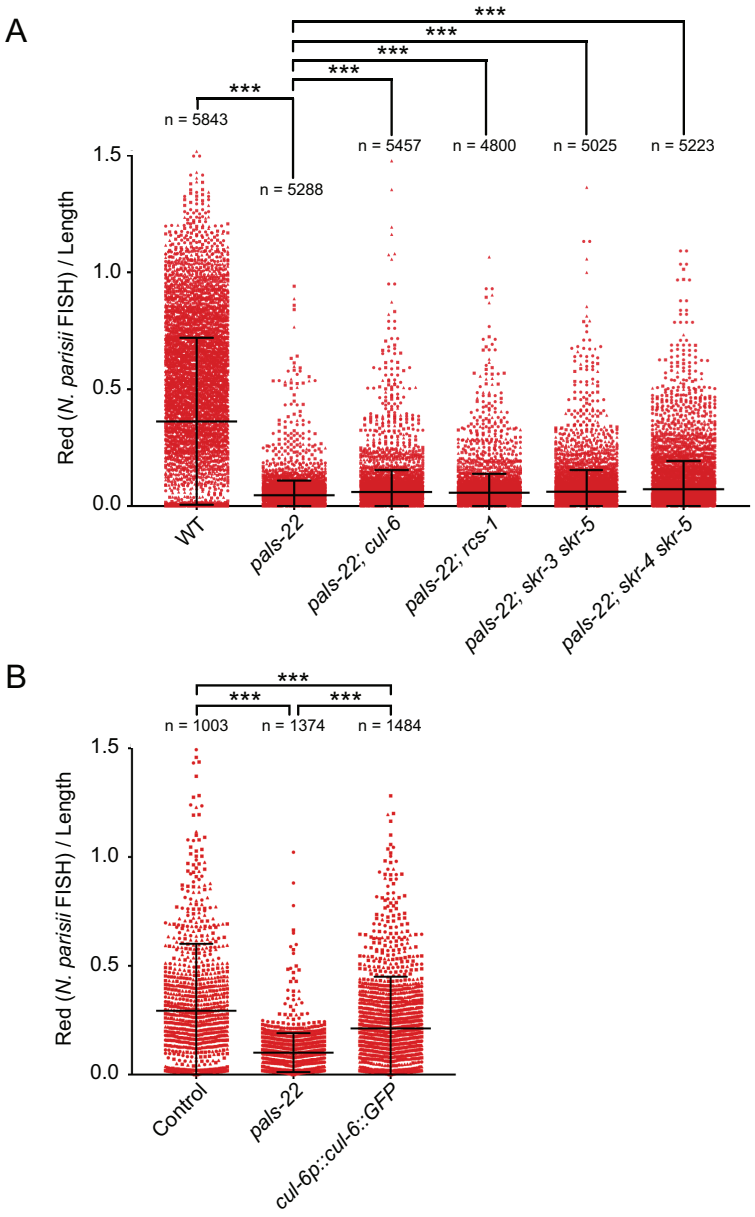

Fig. S6. The CUL-6 ubiquitin ligase complex has a modest role in intracellular pathogen resistance. *(A)* Analysis of pathogen resistance for *cul-6*, *rcs-1* and *skr* double mutants in a *pals-22* background. SCF ligase component mutants in a *pals-22* background are approximately 5-8% more infected than *pals-22* animals. *** $P < 0.001$, Student's t-test as compared to *pals-22* mutants. Error bars indicate mean and SD. *(B)* Analysis of pathogen resistance for *cul-6* ectopic expression in *cul-6p::cul-6::GFP* animals compared to control animals (the unrelated *F42A10.5::GFP* strain was chosen as a negative control, because it contains a Transgeneome construct in an *unc-119* mutant background, like the *cul-6p::cul-6::GFP* strain, and ectopically expresses GFP in the intestine), and *pals-22* mutants. *cul-6p::cul-6::GFP* animals are approximately 27% less infected than control animals but are significantly more infected than *pals-22* mutants. *** $P < 0.001$, Kruskal-Wallis test with Dunn's multiple comparisons test. For *(A)* and *(B) N. parisii*-specific FISH probe (red) was quantified using a COPAS Biosort machine as mean red fluorescence normalized by length of individual animals. Strains were tested in triplicate infection experiments, three plates per experiment, approximately 1200 animals per plate. Each dot represents an individual animal and different shapes represent infection experiments conducted on different days. The number of animals analyzed across three separate infections is indicated for each strain.

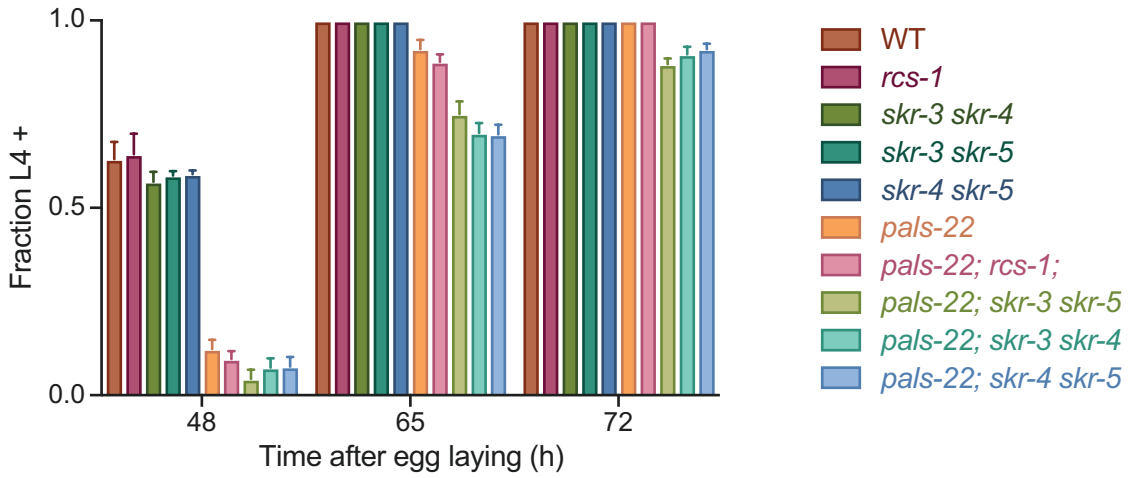

Fig. S7. Analysis of developmental timing for *pals-22*, *rcs-1* and *skr* mutants. *rcs-1* mutants and *skr* double mutants in a *pals-22* background do not suppress the developmental delay of *pals-22* mutants. The fraction of animals reaching the L4 larval stage at time points after eggs were laid is indicated. Results shown are the average of 3 independent biological replicates, with 100 animals assayed in each replicate.

Table S1. List of *C. elegans* strains used in this publication.

Strain Name	Genotype (transgene or mutant allele details)	Source
N2	wild-type	Caenorhabditis Genetics Center
EG6699	*ttTi5605 II; unc-119(ed3) III*	(Frøkjær-Jensen *et al.*, 2012)
RB2266	*skr-5(ok3068) V*	Caenorhabditis Genetics Center
ERT54	*jyIs8[pals-5p::GFP; myo-2::mCherry] X*	(Bakowski *et al.*, 2014)
ERT356	*pals-22(jy1) III*	(Reddy *et al.*, 2017)
ERT365	*unc-119(ed3) III; jyEx193[pals-22::EGFP::3xFLAG, unc-119(+)]*	(Reddy *et al.*, 2017)
ERT413	*jySi21[pET555(spp-5p::strepII3xFLAG_GFP::let858 3'UTR; unc-119(+))] II; unc-119(ed3) III*	This paper
ERT422	*unc-119(ed3) III; jyEx224[cul-6::EGFP::3xFLAG, unc-119(+)]*	(Reddy *et al.*, 2017)
ERT441	*pals-22(jy1) III; cul-6(ok1614) IV*	(Reddy *et al.*, 2017)
ERT443	*jySi22[pET592(myo-2p::GFP::APX_NLS::unc-54; unc-119(+))] II; unc-119(ed3) III*	(Reddy *et al.*, 2017)
ERT465	*unc-119(ed3) III; jyEx237[pals-25::EGFP::3xFLAG, unc-119(+)]*	(Reddy *et al.*, 2019)
ERT479	*pals-22(jy3) III; skr-4(gk759439) V*	(Reddy et al., 2017)
ERT488	*unc-119(ed3) III; jyEx253[F42A10.5::EGFP::3xFLAG, unc-119(+)]*	(Reddy *et al.*, 2017)
ERT554	*pals-22(jy1) III; skr-3(ok365) V*	(Reddy *et al.*, 2017)
ERT555	*pals-22(jy1) III; skr-5(ok3068) V*	(Reddy *et al.*, 2017)
ERT571	*jySi42[pET499(vha-6p::GFP::cul-6::unc-54 3' UTR, unc-119(+))] II; unc-119(ed3) III*	This paper
ERT638	*jySi42 II; unc-119(ed3) pals-22(jy1) III; cul-6(ok1614) IV*	This paper
ERT691	*rcs-1(jy84) X*	This paper
ERT692	*pals-22(jy1) III; rcs-1(jy84) X*	This paper
ERT694	*skr-3(ok365) skr-5(ok3068) V*	This paper
ERT717	*skr-3(ok365) skr-4(gk759439) V*	This paper
ERT718	*skr-5(ok3068) skr-4(gk759439) V*	This paper
ERT720	*pals-22(jy1) III; skr-3(ok365) skr-4(gk759439) V*	This paper
ERT721	*pals-22(jy1) III; skr-3(ok365) skr-5(ok3068) V*	This paper
ERT722	*pals-22(jy1) III; cul-6(ok1614) IV; rcs-1(jy84) X*	This paper
ERT723	*rcs-1(jy105) X*	This paper
ERT724	*pals-22(jy1) III; rcs-1(jy105) X*	This paper
ERT727	*pals-22(jy1) III; skr-5(ok3068) skr-4(gk759439) V*	This paper
ERT739	*jySi45[pET686(myo-2p::GFP::cul-6::unc-54 3' UTR, unc-119(+))] II; unc-119(ed3) III*	This paper
ERT740	*jySi46[pET688(vha-6p::GFP::cul-6(K673R)::unc-54 3' UTR, unc-119(+))] II; unc-119(ed3) III*	This paper
ERT741	*jySi45 II; pals-22(jy1) unc-119(ed3) III; cul-6(ok1614) IV*	This paper
ERT742	*pals-22(jy1) III; cul-6(ok1614) IV; rcs-1(jy105) X*	This paper
ERT752	*jySi46 II; pals-22(jy1) unc-119(ed3) III; cul-6(ok1614) IV*	This paper
ERT817	*jySi42 II; unc-119(ed3) III; skr-3 (ok365) skr-5 (ok3068) V*	This paper
ERT819	*unc-119(ed3) III; jyEx286[pET711(rcs-1::EGFP::3xFLAG, unc-119(+))]*	This paper
ERT820	*unc-119(ed3) III; jyEx287[pET561(skr-5::EGFP::3xFLAG, unc-119(+))]*	This paper
ERT848	*fbxa-75(jy143) III*	This paper
ERT849	*fbxa-75(jy144) III*	This paper
ERT850	*jySi42 II; fbxa-75(jy143) unc-119(ed3) III*	This paper
ERT851	*jySi42 II; fbxa-75(jy144) unc-119(ed3) III*	This paper
ERT852	*fbxa-158(jy145) II*	This paper
ERT853	*fbxa-158(jy146) II*	This paper
ERT854	*fbxa-158(jy145) II; pals-22(jy1) III*	This paper
ERT855	*fbxa-158(jy146) II; pals-22(jy1) III*	This paper

Table S2. List of DNA constructs used in this publication.

Construct Name	Genotype (transgene or mutant allele details)	Source
pET499	*vha-6p::SBP_3xFLAG_GFP_cul-6::unc-54 3'UTR* in pCFJ150	This paper
pET555	*spp-5p::strepII3xFLAG_GFP::let-858-3UTR* in *pCFJ150*	This paper
pET686	*myo-2p::SBP_3xFLAG_GFP_cul-6::unc-54 3'UTR* in pCFJ150	This paper
pET687	*myo-3p::SBP_3xFLAG_GFP_cul-6::unc-54 3'UTR* in pCFJ150	This paper
pET688	*vha-6p::SBP_3xFLAG_GFP_cul-6(K673R)::unc-54 3'UTR* in pCFJ150	This paper
pCFJ150 - Addgene Plasmid #19329	*pDESTttTi5605[R4-R3]*	(Frøkjær-Jensen *et al.*, 2012)
pCFJ601 - Addgene Plasmid #34874	*eft-3p::Mos1* transposase	(Frøkjær-Jensen *et al.*, 2012)
pMA122 - Addgene Plasmid #34873	*peel-1* negative selection	(Frøkjær-Jensen *et al.*, 2012)
pGH8 - Addgene Plasmid #19359	*rab-3p::mCherry*	(Frøkjær-Jensen *et al.*, 2012)
pCFJ90 - Addgene Plasmid #19327	*myo-2p::mCherry*	(Frøkjær-Jensen *et al.*, 2012)
pCFJ104 - Addgene Plasmid #19328	*myo-3p::mCherry*	(Frøkjær-Jensen *et al.*, 2012)
873721959883807 G09	*cul-6::EGFP::3xFLAG* Fosmid; *unc-119* selection	(Sarov *et al.*, 2012)
9830596596427236 B12	*pals-22::EGFP::3xFLAG* Fosmid; *unc-119* selection	(Sarov *et al.*, 2012)
18995122782808704 G01	*pals-25::EGFP::3xFLAG* Fosmid; *unc-119* selection	(Sarov *et al.*, 2012)
8218370932910004 G03	*F42A10.5::EGFP::3xFLAG* Fosmid; *unc-119* selection	(Sarov *et al.*, 2012)
2491680425634929 B04	*rcs-1::EGFP::3xFLAG* Fosmid; *unc-119* selection	(Sarov *et al.*, 2012)
5202602939198744 E05	*skr-5::EGFP::3xFLAG* Fosmid; *unc-119* selection	(Sarov *et al.*, 2012)

Table S3. List of qPCR primers used in this publication.

Primer	Sequence (5' to 3')
snb-1 qPCR forward	CCGGATAAGACCATCTTGACG
snb-1 qPCR reverse	GACGACTTCATCAACCTGAGC
hsp-70 qPCR forward	CTTGGTTGGGGGATCAACT
hsp-70 qPCR reverse	TGCTTCGTCTGGATTAATGG
hsp-4 qPCR forward	CATCTCGTGGAATCAACCCT
hsp-4 qPCR reverse	ACTTAGTCATGACTCCTCCG
hsp-16.2 qPCR forward	TGCAGAATCTCTCCATCTGAGT
hsp-16.2 qPCR reverse	TGGTTTAAACTGTGAGACGTTGA
hsp-60 qPCR forward	CAAGGCTCCAGGATTCG
hsp-60 qPCR reverse	AAAGATCGTTGCTCCCG

Dataset S1 (separate file). Statistical analysis of co-IP experiments. Each tab shows the results for one experimental IP, CUL-6, PALS-22 or PALS-25. Each column indicates the fold change or adjusted p-value of the experimental IP relative to either F42A10.5 or GFP control IPs. Proteins indicated as "TRUE" were significantly more abundant in the experimental IP compared to the control IPs (adjusted $P < 0.05$ and log2 fold change > 1).

References:

1. C. Frøkjær-Jensen, M. W. Davis, M. Ailion, E. M. Jorgensen, Improved Mos1-mediated transgenesis in *C. elegans. Nat. Methods* **9**, 117–118 (2012).

2. M. Bakowski, et al., Ubiquitin-Mediated Response to Microsporidia and Virus Infection in *C. elegans. PLoS Pathog.* **10** (2014).

3. K. C. Reddy, et al., An Intracellular Pathogen Response Pathway Promotes Proteostasis In *C. elegans. Curr. Biol.* (2017) https:/doi.org/10.1016/j.cub.2017.10.009 (August 28, 2017).

4. K. C. Reddy, et al., Antagonistic paralogs control a switch between growth and pathogen resistance in *C. elegans. PLoS Pathog.* **15**, e1007528 (2019).

5. M. Sarov, et al., A genome scale resource for *in vivo* tag-based protein function exploration in *C. elegans. Cell* **150**, 855–866 (2012).